EXPERIMENTAL INVESTIGATION OF THERMOPHYSICAL PROPERTIES OF ENHANCED NITRATE SALT NANOFLUIDS FOR THERMAL ENERGY STORAGE (TES) IN CONCENTRATED SOLAR POWER (CSP) SYSTEMS

by

VAMSIKIRAN ERUVARAM

Presented to the Faculty of the Graduate School of

The University of Texas at Arlington in Partial Fulfillment

of the Requirements

for the Degree of

MASTER OF SCIENCE IN MECHANICAL ENGINEERING

THE UNIVERSITY OF TEXAS AT ARLINGTON

MAY 2018

Acknowledgements

I would like to begin this acknowledgement section by saying a big heart-full thank you to Dr. Donghyun Shin for accepting me as his student in Nanomaterial Research Laboratory. I would like to thank all my laboratory research mates for teaching and helping me in my research work.

I would like to dedicate this thesis work to my beloved father, E.Surendra Reddy – who constantly motivated me up and made me realize the value of education and hard work; my dear mother, K.Chamundeswari, who loved and cared the most for me and to my sweet understanding sister E.Madhuri Mounika and my brother in-law K.V.Achuth, for without their constant words of support and encouragement I would not have been in a position to complete my work successfully.

May 07, 2018

Abstract

EXPERIMENTAL INVESTIGATION OF THERMOPHYSICAL PROPERTIES OF ENHANCED NITRATE SALT NANOFLUIDS FOR THERMAL ENERGY STORAGE (TES) IN CONCENTRATED SOLAR POWER (CSP) SYSTEMS

Vamsikiran Eruvaram, MS

The University of Texas at Arlington, 2018

Supervising Professor: Donghyun Shin

The main source for energy production right now is from thermal, nuclear energy. But in the near future we might have crisis of coal so we need alternate renewable source for energy production the solution for that is sun, since solar energy is renewable and abundantly available. Concentrated solar power (CSP) technologies is one of the best solution to overcome this energy crisis, because it works from solar energy. If the CSP is incorporated with thermal energy storage (TES) we can produce energy even during night. TES with 15-hour storage capacity (Gemasolar) is already commercialized to operate a CSP plant for 24 hours a day. When the sunlight is concentrated by mirrors into a small focal point, a heat transfer fluid transfers the collected heat to a turbine or an engine to produce electricity and any surplus heat to a TES unit for later use. Typical CSP plants used two different materials for heat transfer fluid and TES, and thus several heat exchangers were necessary between HTF and TES. These heat exchangers can cause a significant temperature drop due to the thermal heat transfer losses because of this efficiency of the cycle gets reduced. Thermo physical properties of the HTF are one of the important factors in transferring thermal energy. Different specific heat measurement techniques have been determined in this work for finding the optimum method for Cp measurement. One of the promising chemicals for the purpose of HTF is

mixture of molten salts. However, low thermal properties of molten salts, such as specific heat capacity (Cp around 1.5 kJ/kg°C) constrains thermal performance of CSP systems. Recently, many studies have been conducted to overcome this difficulty, by adding minute concentration of nanoparticles. In this work, the selected molten salt eutectic is a mixture of LiNO3– NaNO3 by composition of (54:46 mol. %) plus dispersing Aluminium oxide (Al2O3) nanoparticles with 40nm particle size. A standard differential scanning calorimeter (SDSC) is employed to measure the Cp of pure and nanomaterial samples. The results from this work shows a 18.3% Cp enhancement. Economic analysis of CSP has been performed to know the effect of impact of specific heat enhancement on CSP by using System Advisor Model as base tool for simulation.

Table of Contents

List of Illustrations

List of Tables

Chapter 1

INTRODUCTION

1.1 Introduction to Specific Heat

Latent heat storage systems have gained importance for many applications like space-based power plants, solar energy systems, and central air-conditioning systems and in energy-conserving buildings, due to their high energy density and isothermal behavior during charging and discharging [6]. The most difficult part of this is their selection or preparation of a suitable phase-change material (PCM) for a heat storage system. Specific heat describes the amount of heat per unit mass required to raise the temperature by one degree [2]. Some of the techniques discussed here for specific heat measurement are Modulated differential scanning calorimetry (MDSC), standard differential scanning calorimetry(SDSC) and T history method.

1.2 Introduction to DSC

Differential scanning calorimetry (DSC) is a thermal analysis technique which has been used for more than two decades to measure the temperatures and heat flows associated with transitions in materials as a function of time and temperature. Such measurements provide quantitative and qualitative information about physical and chemical changes that involve endothermic or exothermic processes, or changes in heat capacity. DSC is the most widely used thermal analysis technique with applicability to polymers and organic materials, as well as various inorganic materials. DSC has many advantages which contribute to its widespread usage, including fast analysis time (usually less than 30 minutes), easy sample preparation, applicability to both solids and liquids, wide temperature range, and excellent quantitative capability[1].

1.2.1 Working DSC:

In a typical heat-flux DSC cell, the sample and reference sit on raised platforms formed in a thermoelectric disk, which serves as the primary means of heat transfer to the sample and reference from a temperature-programmed furnace. Traditionally, the temperature of the furnace is raised or lowered in a linear fashion, while the resultant differential heat flow to the sample and reference is monitored by plate thermocouples fixed to the underside of the disk platforms. The thermocouples are connected in series and measure the differential heat flow using the Ohm's Law[2]

$$dQ=\frac{dT}{R}$$

dQ= difference in heat flow between sample and reference,

dT= temperature difference measured,

R = thermal resistance of the cell.

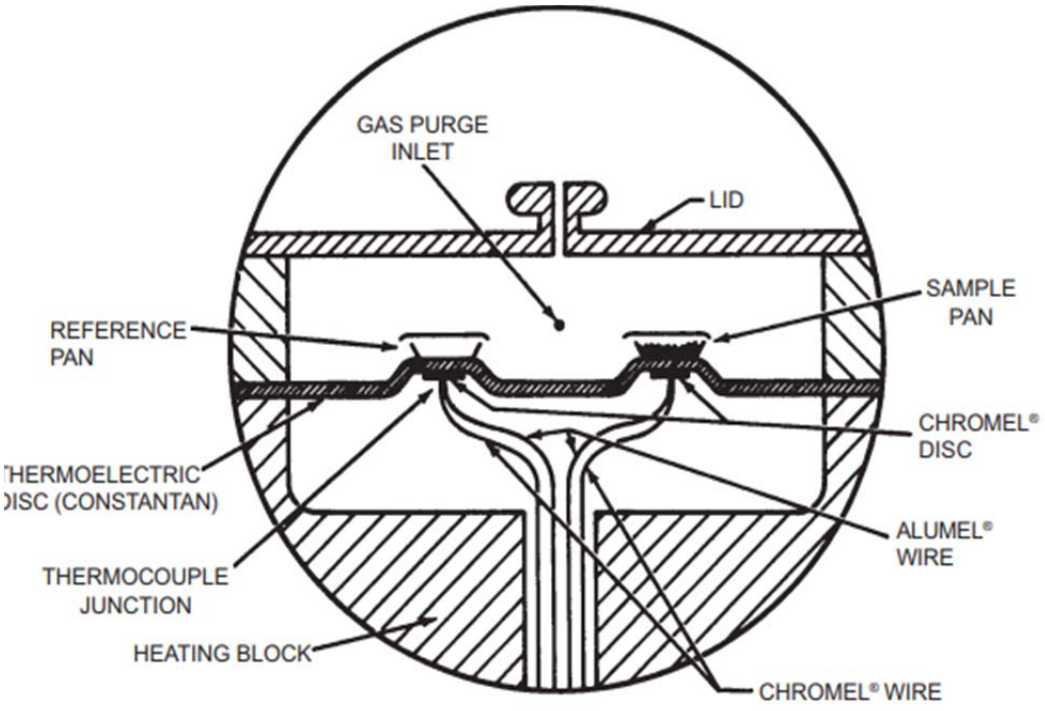

Figure1.1 Heat flux DSC Schematic[4]

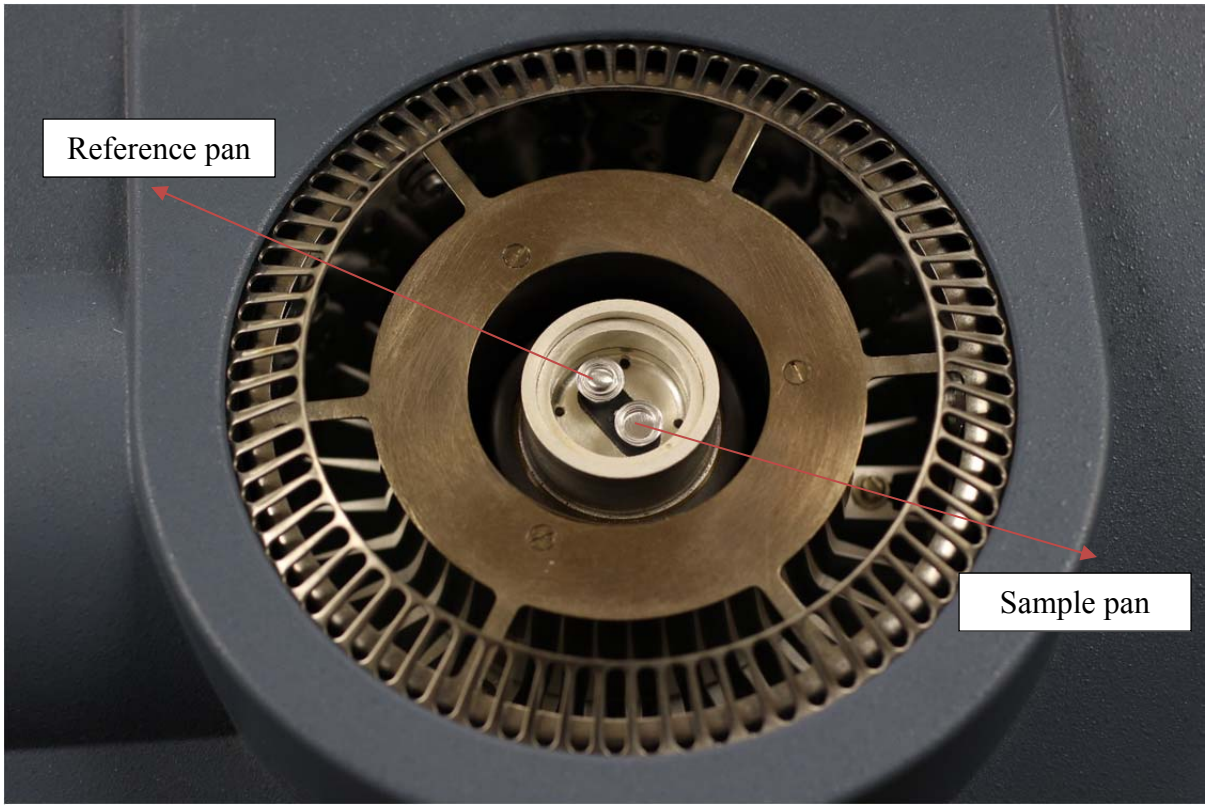

Figure1.2 Heat flux DSC Texas instruments

In modulated DSC (MDSC), the same heat-flux DSC cell arrangement is used as that of standard DSC, but a different temperature (heating/cooling) profile is applied to the sample and reference via the furnace. Specifically, a sinusoidal ripple (modulation) is overlaid on the standard linear temperature ramp. Due to this, there are three heating-related experimental variables, which can be used to improve DSC results. These three variables are heating rate, amplitude of modulation, and frequency of modulation. To appreciate the effects these variables can have, the general equation describing calorimeter response needs to be examined. One way to represent this heat flow mathematically is[5]

$$dQ/dt = -\frac{dT}{dt}\,[C_p + f'(t, T)] + f(t, T)$$

dQ/dt = heat flow out of the sample,

dT/dt = heating rate,

Cp = sample heat capacity,

t = time,

T = temperature,

f''(t, T) = thermodynamic heat flow component,

f(t, T) = kinetically-limited heat flow

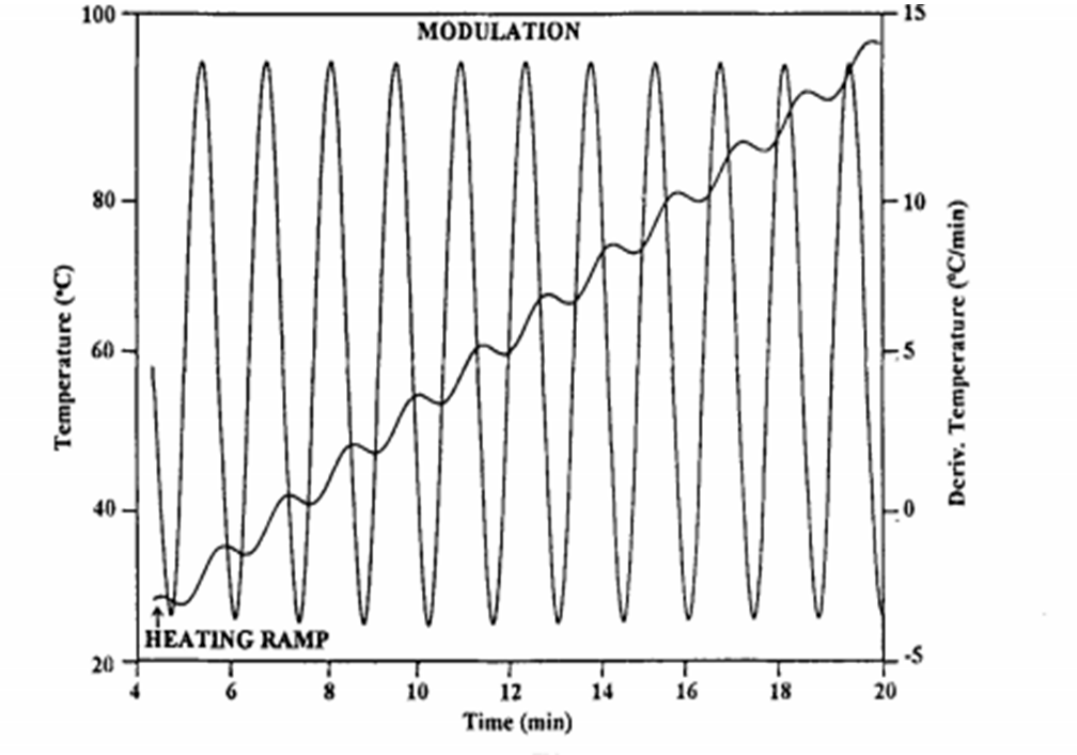

Figure 1.3 Modulated DSC heating profile [5]

1.3 Introduction to T-History

T history method works on the principle of lumped heat capacitance method. For heat conduction in a solid body there are two thermal resistances: (1) the conductive

thermal resistance R_K inside (2) the convective thermal resistance R_C between the surface of the solid body and the neighboring fluid. An important limiting case relates to negligible conductive thermal resistance $R_K \rightarrow 0$ or alternatively $R_K << R_C$, in which there is a small temperature difference between the center and the surface in the solid body and a large temperature difference between the surface and the adjacent fluid. The unsteady heat conduction takes place in a "lumped" solid body whose mean temperature depends on time. This hypothesis gives rise to the powerful lumped capacitance model. The lumped capacitance model is a natural branch of the differential or distributed model in which the temperature in the solid body depends upon position and time unitedly. Lumped heat capacity is valid only when Bi<<1 [21, 22]

$$\text{Bi}=\frac{R_K}{R_C}<<1.$$

1.4 Introduction to Solar Energy

The main sources of energy production are crude oil, gas and coal. According to a model developed by Klass it is estimated that coal reserves are available up to 2112[6]. Wind Energy, Geothermal Energy, Solar Energy, Hydropower, Biomass Energy, Biodiesel and Advanced Biofuels are some of the example of renewable energy on the surface of earth. Solar Energy stands out. 400, 000, 000, 000, 000, 000, 000, 000, 000 watts of energy is produced by sun [chenglu1], it is estimated that it will last for around 5 billion years. The two technologies that is used for the production of electricity from sun are photovoltaic and concentrated solar power plant.

1.4.1 Photovoltaic Technology

The semiconductor device that transforms solar light in electrical energy is termed as 'Photovoltaic cell' , Solar cells are made of semiconductor materials, such as silicon. The solar cells has a thin semiconductor wafer to form an electric field, P type semiconductor on one side and N type on the other. When light energy (sunrays) strikes the solar cell, electrons are knocked out from the atoms in the semiconductor material producing electricity. The main advantage of this system is easy to install , easier conversion of solar energy , but the disadvantage with this technology is cost of production of electricity and its operational time.[7,8],The photovoltaic system works only in the presence of sun light , the electricity production cannot be done in the absence of the sunlight. In order to overcome this limitation concentrated solar power plants can be used.

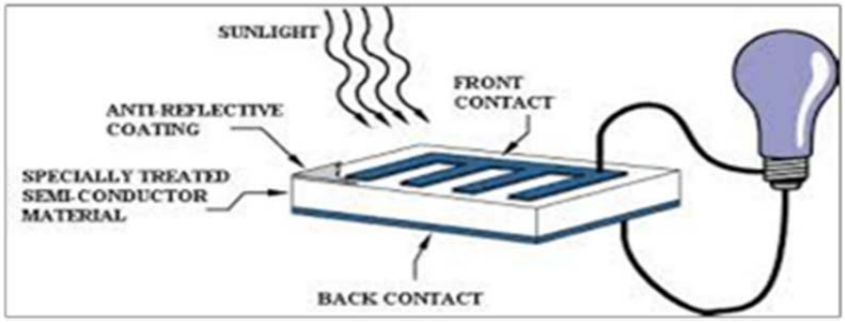

Figure1.4 Photo voltaic cell working [9]

1.4.2 Concentrated solar power plant

CSP use an array of mirror as optical elements which are used to concentrate solar energy and convert them to thermal energy [10]. The operating temperatures of these plants are around 300^0C – 600^0C. Thus using CSP, the energy is stored in the thermal energy storage tanks and then this energy is used to drive the generator, which produces electricity. CSP has four technologies that are used to produce electricity namely

Parabolic Trough Systems, Concentrated Solar Power tower, Fresnel Linear Technology and Dish stirling.

1.4.2.1 Parabolic Trough System

This system has cylindrical and parabolic reflector, which is used to focus the sun's radiation on to a vacuumed glass tube. The vacuum tube consists of absorption tube which is used to absorb the heat from the sun's energy this absorption tube has high absorptivity and low emissivity, this property helps in reduction of heat loss. High temperature fluid or heat transfer fluid is allowed to flow inside the absorption tube, which gets heated up by absorbing heat reflected by the reflectors. The heat transfer fluid generally used in this system is mineral oil. This system can reach up to temperature of 400^0C. The heated fluid is transferred to heat exchanger by pumps and in the heat exchanger heat transfer takes place and converts into steam. The steam generated is used to run the turbines to produce electricity.

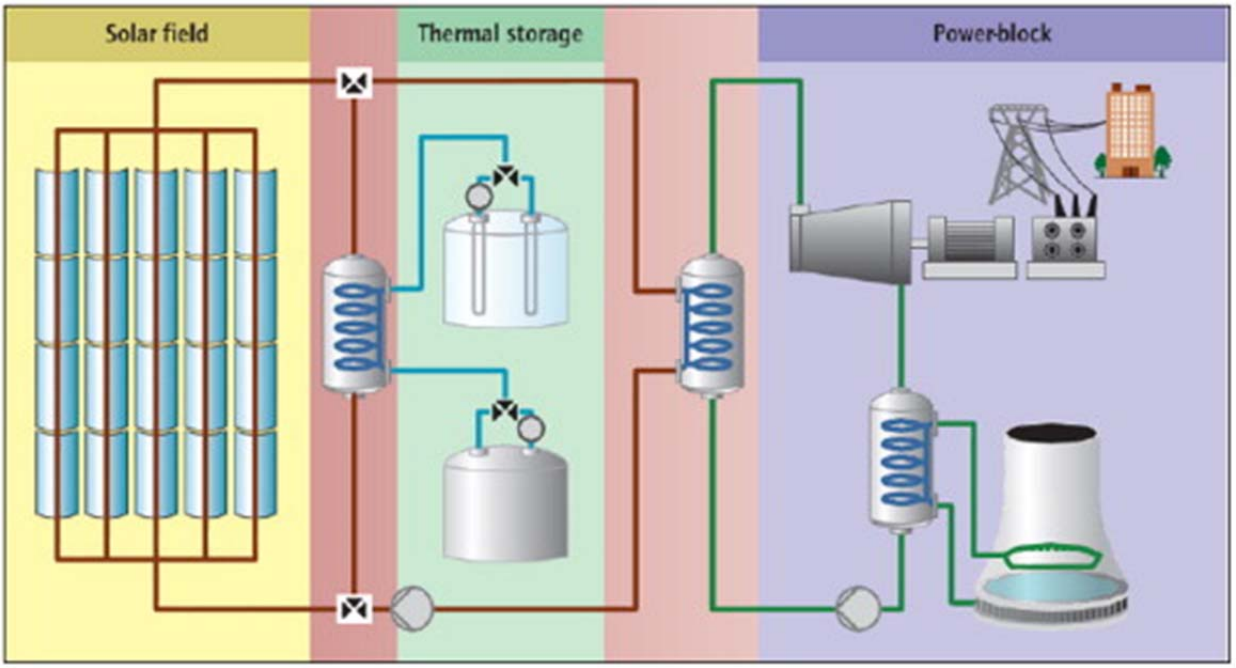

Figure 1.5 Parabolic trough system [11]

1.4.2.2 Power Tower

This system consists of several reflecting mirrors called as heliostats. The heliostats have a surface area of around 100m^2 on average. The heliostats are mounted around a central receiver in which high temperature fluid is allowed to flow which could be a molten salt, like liquid water, air or sodium in liquid state. These heliostats are has its own sun tracking system along two axis. The heliostats are usually flat. The receiver is usually located on to a tower, which is around 80m – 100m in height. The main advantage of having a solar power tower is it's point focus system which is good when compared to line focusing as that of parabolic trough system. Huge amount of radiation is allowed to focus on to the receiver, which is helpful in increasing the efficiency of the system and also it reduces the heat losses, due to this we can increase the operating temperature of plant which increases the efficiency of Rankine cycle.

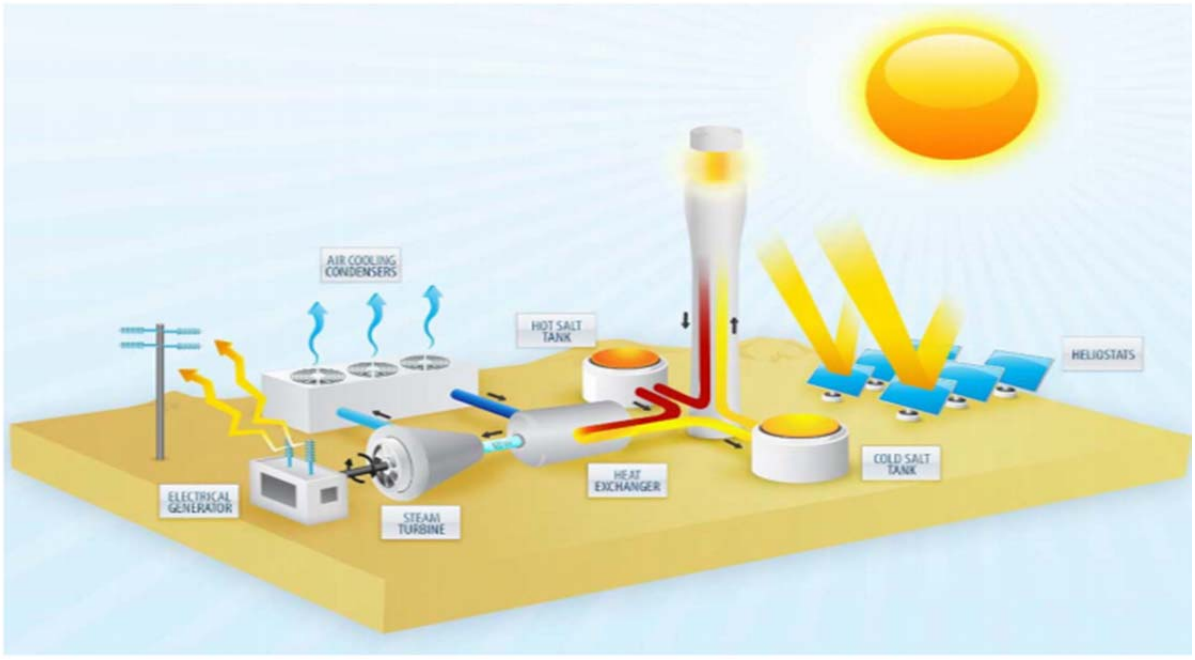

Figure 1.6 Power tower system [12]

1.4.2.3 Fresnel Linear Technology

Fresnel Linear system consists of mirrors, which can be parabolic or flat in shape. The mirrors are used to reflect the sun's irradiation on to towards the tube. The tubes contain water running in it. The water is heated and it's converted to steam. This pressure created by steam is used to run the turbine to produce electricity.

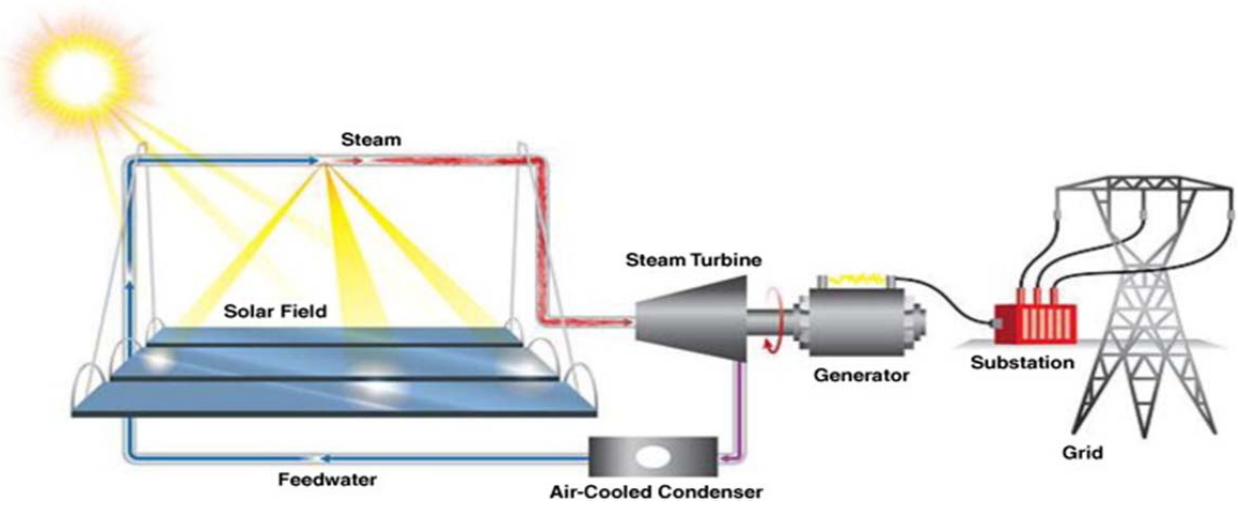

Figure 1.7 Fresnel System [13]

1.4.2.4 Dish stirling Technology

Dish stirling is point focus system. This system consists of parabolic shaped dish, which reflects the sun's radiation to a single receiver; the single receiver is this is stirling engine, which is heat engine. The stirling engine generally absorbs heat energy and converts it to mechanical work. In this system, a parabolic shaped dish is used to reflect sun's radiation on to a single receiver, which in this case is a Stirling engine, which is nothing but a heat engine. An alternator attached to the engine shaft, which converts mechanical work to electricity. Parabolic dishes are usually coated with reflective material such glass, aluminum, plastic.

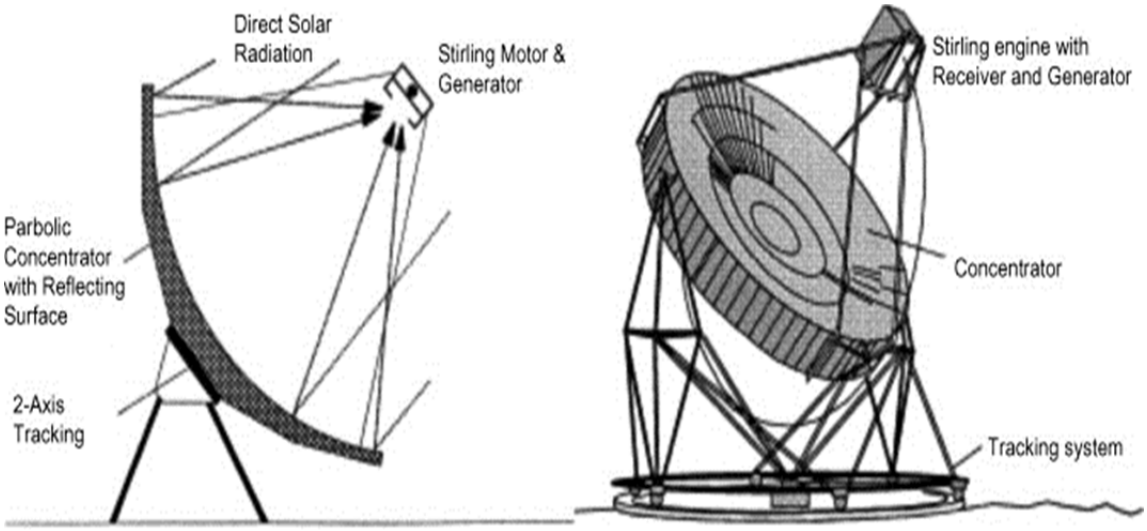

Figure 1.8 Dish stirling system [13]

1.5 Thermal Energy Storage System and energy storage systems

The sun energy is only available during the daytime but not the night or in some cloudy conditions. This is one of the difficulty associated with the use of solar energy to produce electricity, to encounter this problem we need an energy storage system which can store energy during the daytime and can be used when required. Energy storage systems are divided in to three categories namely sensible heat storage system, Latent heat storage system and chemical energy storage.

1.6 Eutectic nitrate/nitrite mixture

Eutectic mixture of $LiNO_3$ and $NaNO_3$ are used here attributing to their low melting point. At present the industrial energy storage material, which is binary mixture of KNO_3 and $NaNO_3$ also known, has solar salt, has freezing point of 222^0C. Various methods such as circulating heat transfer fluid during the nighttime through solar field and using auxiliary heater to maintain certain temperature are used to prevent freezing of salt.

1.7 Introduction to SAM and Gemasolar plant

SAM is developed by the national renewable energy laboratory (NREL) with funds from the United States department of energy.. The System Advisor Model (SAM) is a performance and financial model designed to facilitate decision making for people involved in the renewable energy industry. SAM makes performance predictions and cost of energy estimates for grid-connected power projects based on installation and operating costs and system design parameters that you specify as inputs to the model.

Gemasolar, located in Fuentes de Andalucía, Spain, about 40 miles east of Sevilla, is the first commercial-scale plant in the world to apply central tower receiver and molten salt heat storage technology. The plant has a capacity of 19.9 MWe (gross) and covers slightly less than 200 hectares. The Gemasolar power plant consists of 2,650 heliostats distributed in concentric rings around the tower, with a total reflective area of 304,750 m^2, in an immense 185-hectare circle. The 115 m^2 heliostats developed by SENER use proprietary technology to track the sun's location in order to maximize the collection of thermal energy, and their location was established by the SENSOL software. These heliostats reflect and concentrate sun radiation on a 120 MWth [18] solar receiver located on the upper part of 140 m tower. Molten salt is pumped from a cold storage tank through the receiver where is heated and then stored into a hot tank. From the hot tank the salt is pumped to a steam generation system. The superheated steam produced drives a 19.9 MWe (gross) Siemens SST-600 two-cylinder reheat steam turbine, which is connected to a generator that produces electricity. The plant uses a wet-cooling system to condense the steam back to liquid. The Gemasolar power plant has a thermal storage system which stores part of the heat produced in the solar field during the day in a molten salt mixture of 60% sodium nitrate and 40% potassium nitrate [18]. A full storage tank can be

used to operate the turbine for about 15 hours at full-load when the sky is overcast or after sunset. The plant also utilizes a 15% fossil fuel back-up from a natural gas heater.

1.8 Objective of the Study

The aim of this study is to discuss different techniques for the measurement of specific heat, investigate the effect of nanoparticle dispersions on binary nitrate molten salt as advance thermal energy storage material by doping the base nitrate molten salt with Aluminum oxide nanoparticle in very minute concentration, and discuss the economic impact of incorporating nanoparticles in thermal energy storage system by the help of System Advisor Model (SAM).

1.9 Significance of the Study

The significance of this study is to develop advanced nanomaterials for heat transfer and thermal storage applications to be used in CSP. The output from this study support the use of nanomaterials for heat capacity enhancement and act as a potential substitute to the existing heat transfer fluids with a great reduction in cost.

CHAPTER 2

EXPERIMENTAL PROCEDURE

2.1 Synthesizing procedure for solar salt:

A binary eutectic mixture of $NaNO_3$ – KNO_3 is considered here for purpose of study of specific heat of molten salt. The composition, which forms the eutectic mixture of $NaNO_3$ – KNO_3 by mixing is (60-40) in mass fraction (wt. %). The salts used in procedure were procured from Alfa Aesar Corporation. $NaNO_3$, KNO_3 procured were 99.0 % pure of $LiNO_3$, 80 mg of KNO_3 and 120 mg of $NaNO_3$ were mixed using a microbalance (Sartorius, CPA225D). The mixture is prepared in 25 ml glass vial. The glass vial is filled with 20 ml water and allowed to sonicate for 200 minutes in an ultra sonicator (Branson, 1510), procured from Branson Ultrasonic Corporation. The sonication is used to make eutectic mixture. The sonicated vials were evaporated in furnace plate at temperature of 200^0C for 8 hours.

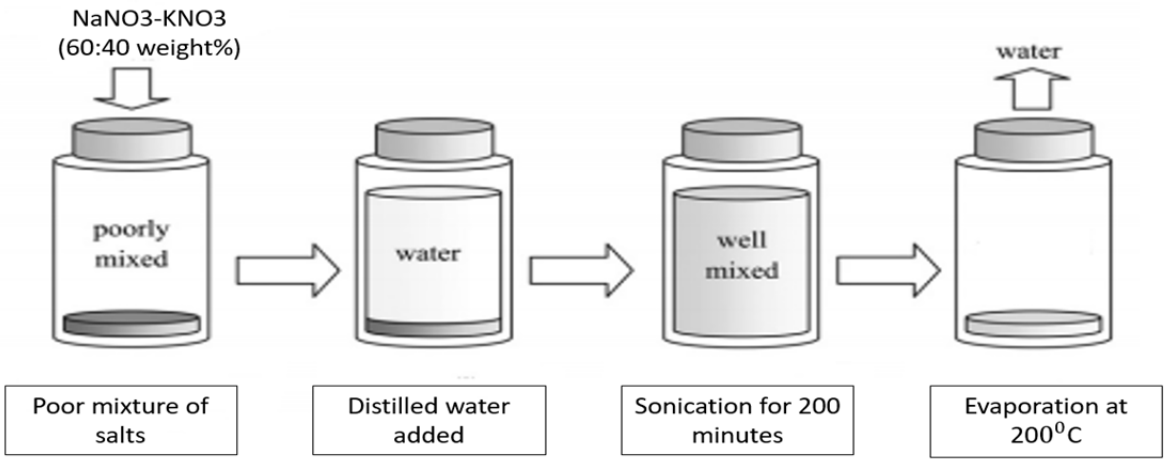

Figure 2.1 Synthesis of Solar Salt [17]

2.2 Synthesizing procedure for pure and nano sample of $LiNO_3$-$NaNO_3$

A binary eutectic mixture of $LiNO_3$- $NaNO_3$ is considered here for purpose of study. The composition, which forms the eutectic mixture of $LiNO_3$ – $NaNO_3$ by mixing is (54:46) in molar mass . The salts used in procedure were procured from Alfa Aesar Corporation. $LiNO_3$ $NaNO_3$ procured were 99.0 % pure. Aluminium oxide (Al_2O_3) nanoparticles used were procured from Meliorum Technology. 40nm. 101.422 mg of $LiNO_3$, 96.577 mg of $NaNO_3$ and 2mg of Al_2O_3 were mixed using a microbalance (Sartorius, CPA225D). The mixture is prepared in 25 ml glass vial. The glass vial is filled with water up to 20 ml and allowed to sonicate for 30 minutes in an ultra sonicator (Branson, 1510), procured from Branson Ultrasonic Corporation. The purpose of the sonication is that all the elements are mixed homogenously for uniform dispersion of the nanoparticles and minimum agglomeration. The sonicated vials were evaporated on hot plate at temperature of 150^0C for 10 hours. After complete removal of water, the remaining solution is allowed to solidify and heated at lower temperature of 100^0C to remove any trace of moisture from the sample.

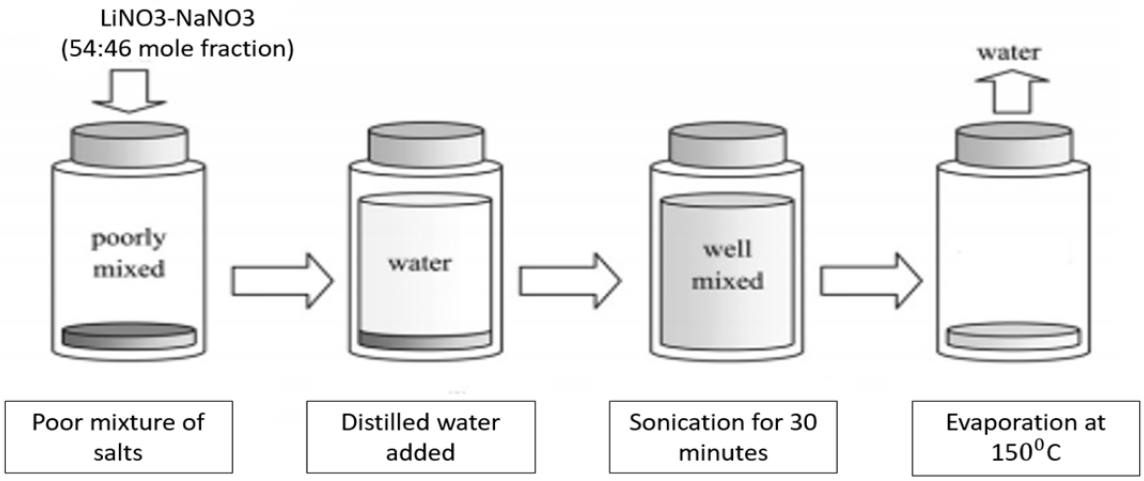

Figure 2.2 Synthesis of Nanomaterial [17]

2.3 Properties of salt used

Table 2.1 Large Table in Landscape Orientation

Properties	Sodium Nitrate	Potassium nitrate	Lithium Nitrate
Molar Mass	84.99gm/ mole	101.1gm/ mole	68.95gm/ mole
Melting Point	306^0C	400^0C	251^0C
Boiling Point	380^0C	334^0C	600^0C
Decomposition Temperature	$>400^0$C	380^0C	$>600^0$C
Flash Point	Nonflammable	Nonflammable	Nonflammable

2.4 Testing procedure in Modulated DSC:

A modulated protocol is used in the Differential Scanning Calorimeter (DSC) to measure the specific heat capacity. Two pans are loaded in MDSC empty pan and sample pan. Three calibrations has to be done before testing the sample namely baseline slope and offset calibration, enthalpy (cell) constant calibration, Heat capacity calibration.

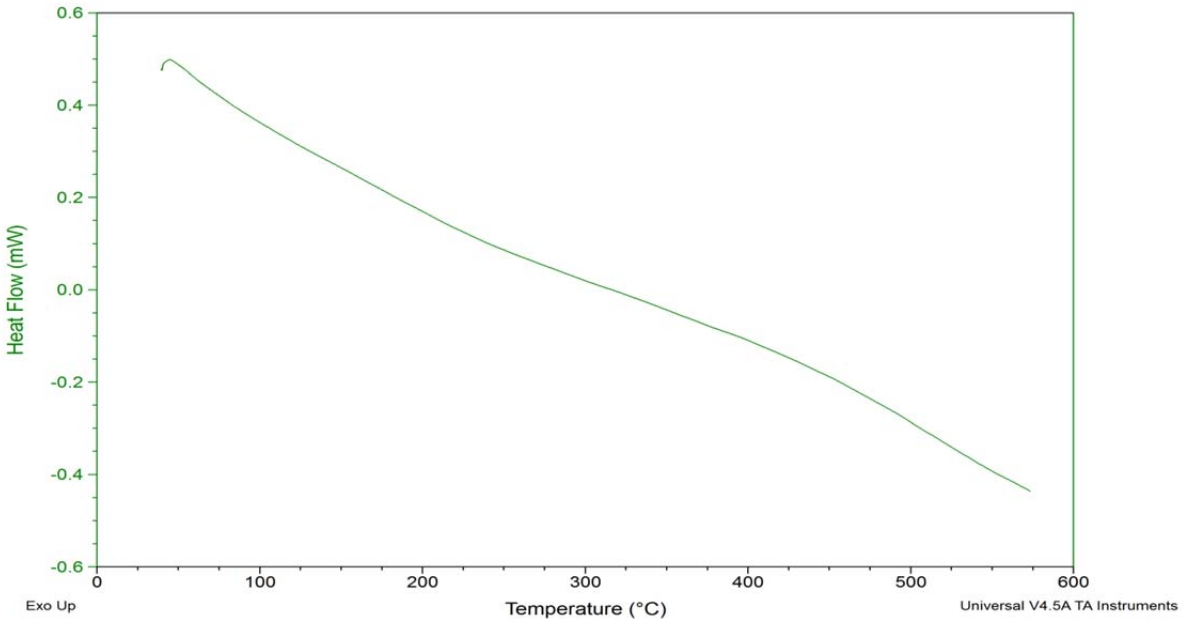

Figure 2.3 baseline slope and offset calibration

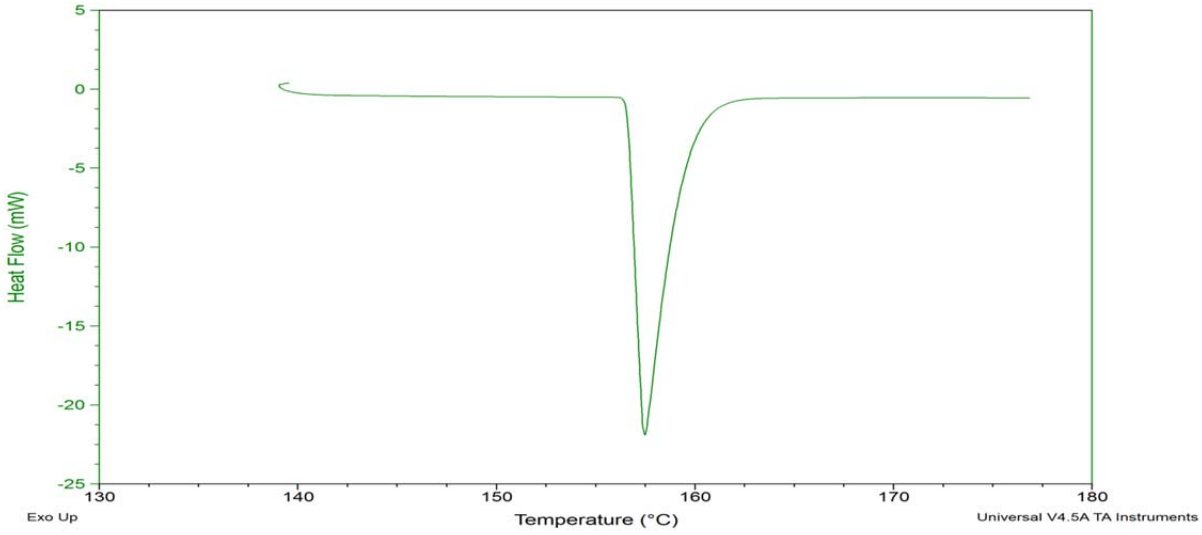

Figure 2.4 Indium for enthalpy (cell) constant calibration

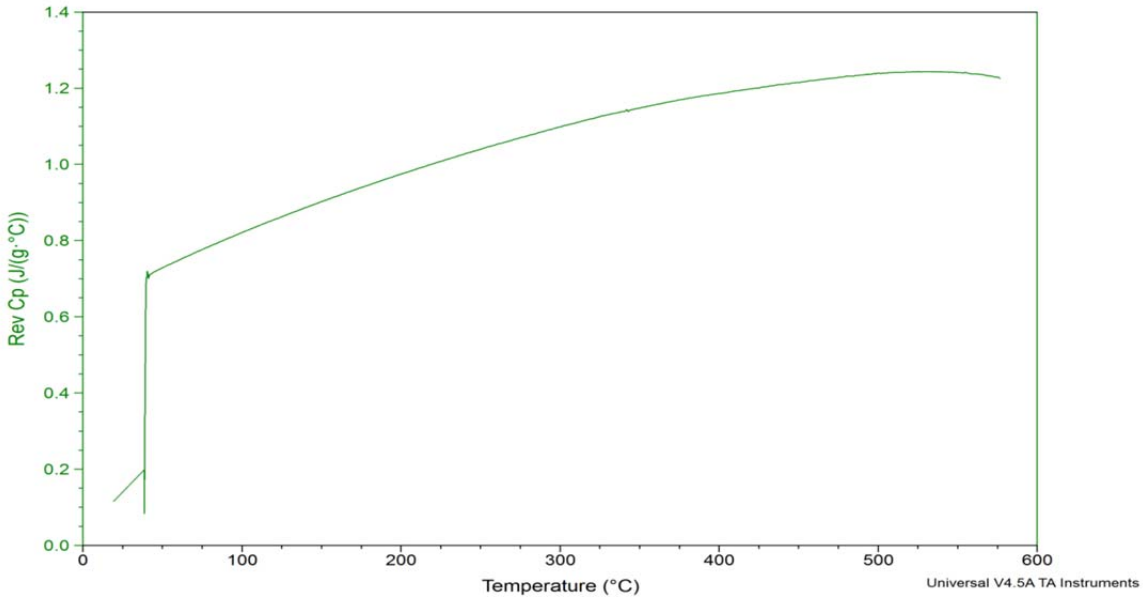

Figure 2.5 Saphire Heat capacity calibration

2.4.1 Protocol is used for testing in MDSC:

The empty pan is used for reference initially the samples are maintained at a temperature of 40^0C and then the temperature is ramped up to 560^0C at the rate of 5^0C/min. The samples are maintained at that temperature for 5 minute i.e. the samples are at isothermal state. Gradually the samples are allowed to cool down. Results of specific heat capacity are obtained from software from TA Universal Analysis (TA Instruments) [17]

2.5 Testing procedure in SDSC:

The standard T-zero hermetic pan was fixed with a lid (TA Instruments, Inc.) and hermetically sealed. Before testing the samples in the pan, the empty pan/lid and the pan/lid with a sapphire reference (25.412 mg) were mounted in a differential scanning calorimeter (Q20, TA Instruments, Inc.) to obtain a baseline and a reference data. The

standard DSC test method (ASTM-E1269) was used for the measurement of specific heat. [23]

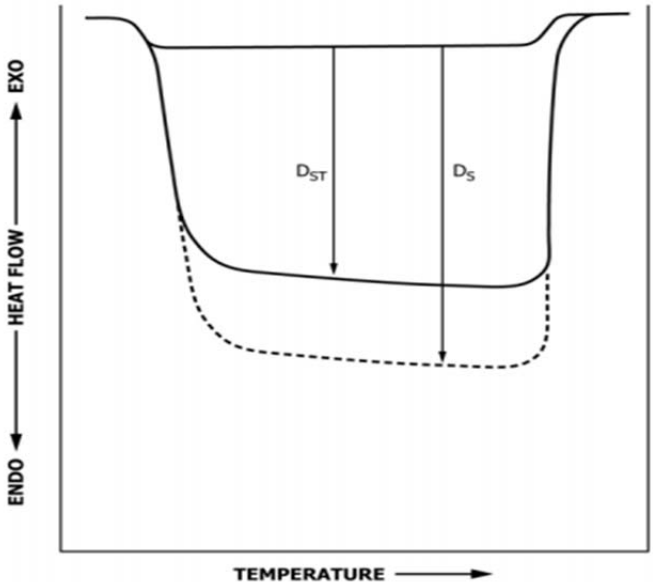

Figure 2.6 SDSC ASTM-E1269 for specific heat measurement [23]

2.5.1 Protocol is used for testing in SDSC:

The temperature was initially held at 150 °C for at least 4 min. to evaporate any adsorbed moisture. The temperature was then ramped up to 560 °C at 20 °C/min. and held for another 4 min. The DSC was then cooled down to room temperature.

2.6 Testing procedure of specific heat by T-History method:

The fundamental of T-history method is the lumped capacitance assumption, in which the conduction within the sample is negligible [21, 22].

$$\mathrm{Bi} = \frac{\mathrm{h_{air}} L_C}{k} = \frac{\mathrm{h_{air}} V_{\mathrm{sample}}}{A_{\mathrm{surface}} k}$$

The volume and height of the sample in the vial is determined by the mass of sample filled. In our setup, 1.0-inch diameter vial was used to carry the salt sample with a height

of 1.25 inch. The characteristic length is calculated to be Volume/Area = 0.178 in = 0.0045 m. Assuming the natural convective heat transfer coefficient to be 5 W/m2-K and thermal conductivity to be 0.5 /m-K, the Biot number is calculated to be 0.045 which meets the lumped capacitance method requirement

Table 2.2 Specifications and considerations for T-History method

Specifications and considerations	
Vial diameter	1 inch
Height of salt in vial	1.25 inch
Volume/Area of Vial	0.178inch
Thermal conductivity	0.5W/m-k
Heat transfer co-efficient	5 W/m^2-K

2.6.1 Validation of temperature distribution:

The validation has been done by using two vials filled with $NaNO_3$ salts with same mass. The samples are heated in furnace from same initial temperature, two set of tests were performed with different initial temperature.

- Equilibrate at 250°C and ramp up to 500°C
- Equilibrate at room temperature (25°C) and ramp up to 500°C

2.6.1.1 Equilibrate at 250°C and ramp up to 500°C:

In this first the salt is allowed to equilibrate at 250^0C and then the temperature is ramped to 500^0C and time Vs temperature is recorded with the help of DAQ

2.6.1.2 Equilibrate at 25°C and ramp up to 500°C:

In this first the salt is allowed to equilibrate at 25^0C and then the temperature is ramped to 500^0C and time Vs temperature readings are recorded with the help of DAQ

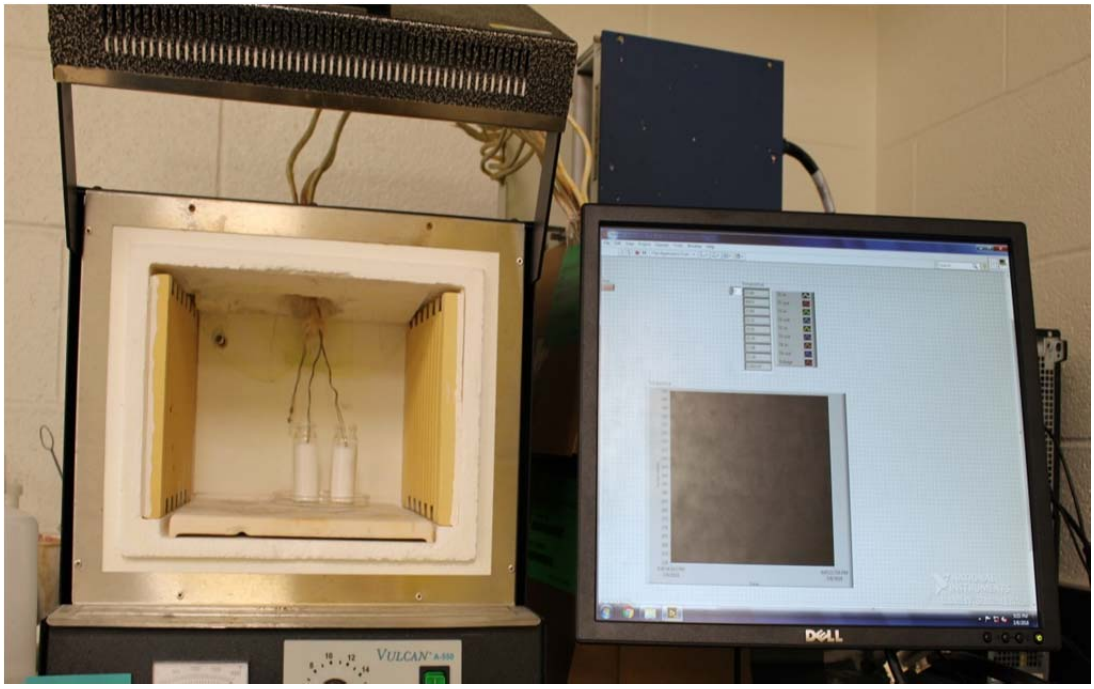

Figure 2.7 T-History experimental setup

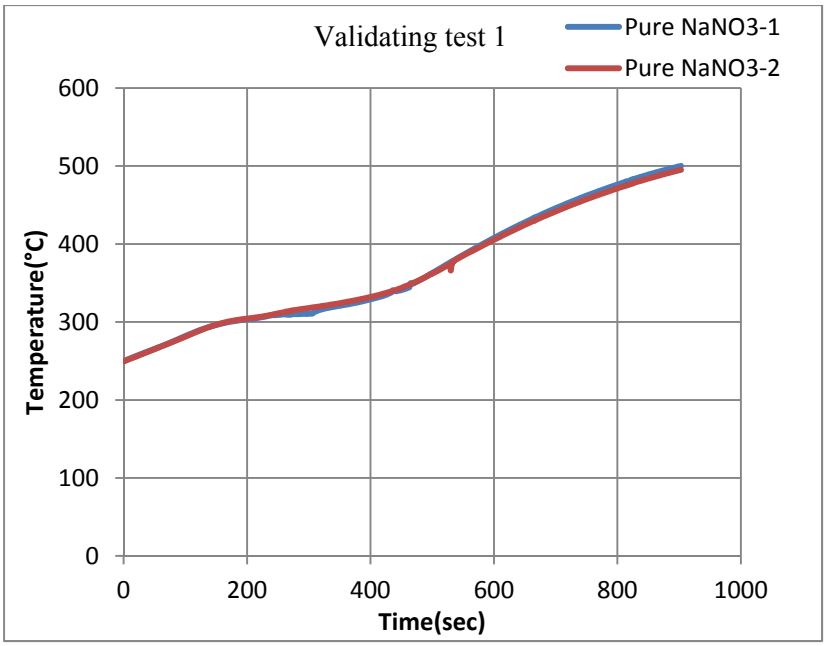

Figure 2.8 Time Vs Temperature for validation-1

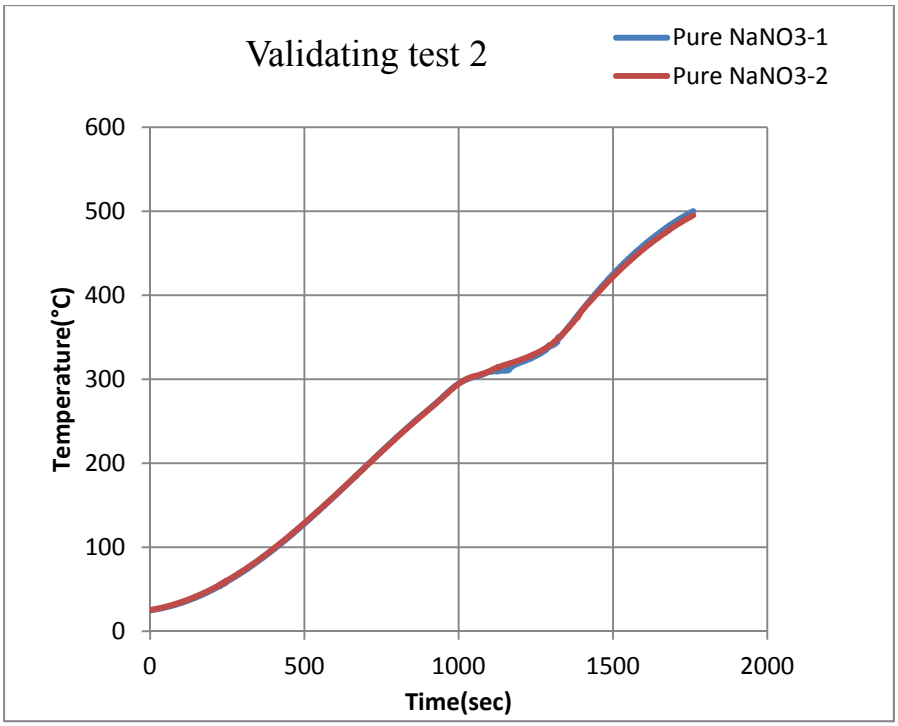

Figure 2.9 Time Vs Temperature for validation-2

2.6.2 Test protocol for T-History method:

30 gms of pure molten solar salt and 30 g of $NaNO_3$ salt were weighed in each vial respectively. Both the samples are placed adjacently inside furnace and allowed to equilibrate at 250°C and then allowed to ramp. The temperature change with respect to time is recorded with the help of K type thermocouples which are hooked to TA data acquisition system; the furnace air temperature is also monitored during the whole process.

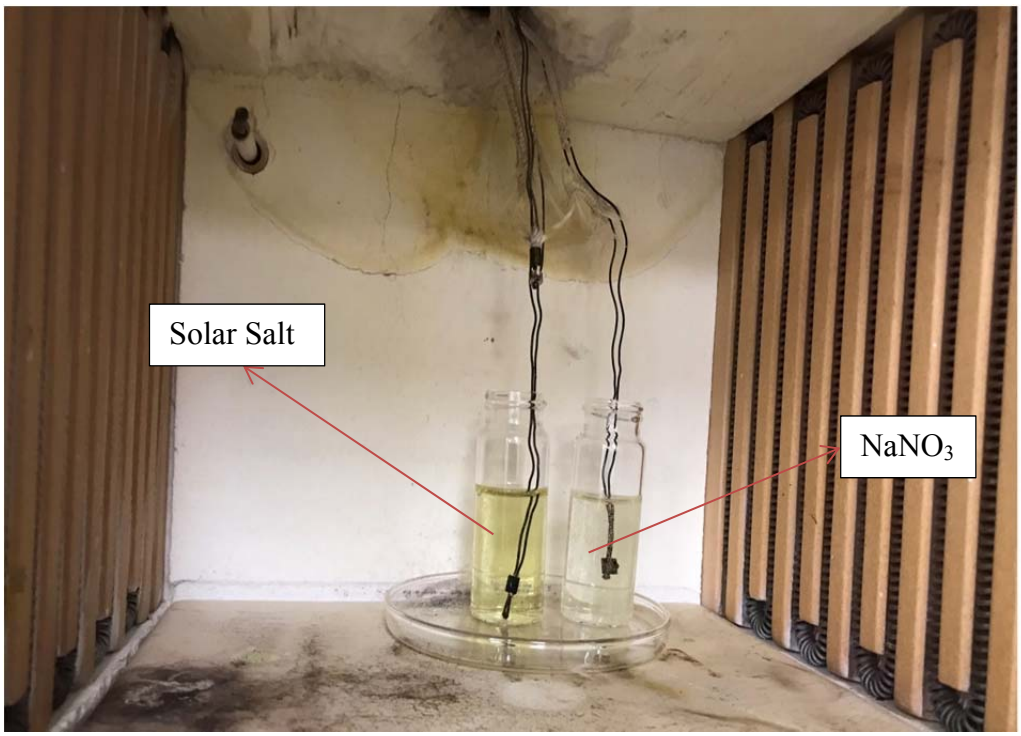

Figure 2.10 Solar slat and $NaNO_3$ after melting

2.7 SAM performance inputs for Gemasolar

Table 2.3 Input parameters of Gemasolar [18]

Parameter	Variable	Gemasolar input
Climate	Location	Sevilla (EPW)
Heliostat Field	Heliostat width	10.9 m
	Heliostat height	10.9 m
	Max heliostat distance to tower	8
	Solar field land area multiplier	1.4
Tower and Receiver	Receiver height	140 m
	Receiver diameter	8.89 m
	Number of panels	16
	Required HTF outlet temp	565 ºC
	Solar multiple	2.5
	Tower height	140 m
Power Cycle	Design turbine gross output	19.9MW
	Estimated gross to net conv	0.875
	Design HTF inlet temperature	565 ºC
	Aux heater outlet set temp	570 ºC
	Min turbine operation	0.20
	Condenser type	Evaporative
	Ambient temp at design	20 ºC
Thermal Storage	Full load hours of TES	15
	Initial hot HTF temp	565 ºC

2.8 HTF parameters for SAM

Parameters like specific heat, kinematic viscosity, dynamic viscosity has been taken from National renewable energy laboratory of the U.S. Department of Energy.

Table 2.4 Input parameters of HTF (Solarsalt) in system advisor model[19]

Temperature [C]	**Specific heat** [kJ/kg-K]	**Dynamic viscosity** [Pa-s]	**Kinematic viscosity** [m^2-s]
260	1.488	0.004343	2.26E-06
277.9	1.491	0.003818	2E-06
295.8	1.494	0.003361	1.77E-06
313.7	1.497	0.002967	1.57E-06
331.6	1.5	0.002629	1.4E-06
349.5	1.503	0.002344	1.26E-06
367.4	1.506	0.002106	1.13E-06
385.3	1.509	0.00191	1.04E-06
403.2	1.512	0.001751	9.55E-07
421.1	1.515	0.001624	8.91E-07
438.9	1.518	0.001523	8.41E-07
456.8	1.522	0.001445	8.03E-07
474.7	1.525	0.001383	7.73E-07
492.6	1.528	0.001332	7.50E-07
510.5	1.531	0.001289	7.30E-07
528.4	1.534	0.001247	7.11E-07
546.3	1.537	0.001201	6.89E-07
564.2	1.54	0.001147	6.62E-07
582.1	1.543	0.001078	6.27E-07
600	1.546	0.000992	5.80E-07
800	1.546	0.000992	5.80E-07

CHAPTER 3

RESULTS AND DISCUSSION

3.1 Specific Heat capacity measurement

3.1.1 Specific heat capacity by MDSC

Table 3.1 Results of Specific heat capacity by MDSC

Heat capacity(kJ/kg°C)	**$NaNO_3$-KNO_3(SOLAR SALT)**	
Heat capacity	**Experimental**	**Reference[20]**
Repeat #1	**1.55**	**1.45-1.55**
Repeat #2	**1.54**	
Repeat #3	**1.56**	
Average	**1.55**	
Standard deviation	**0.01**	

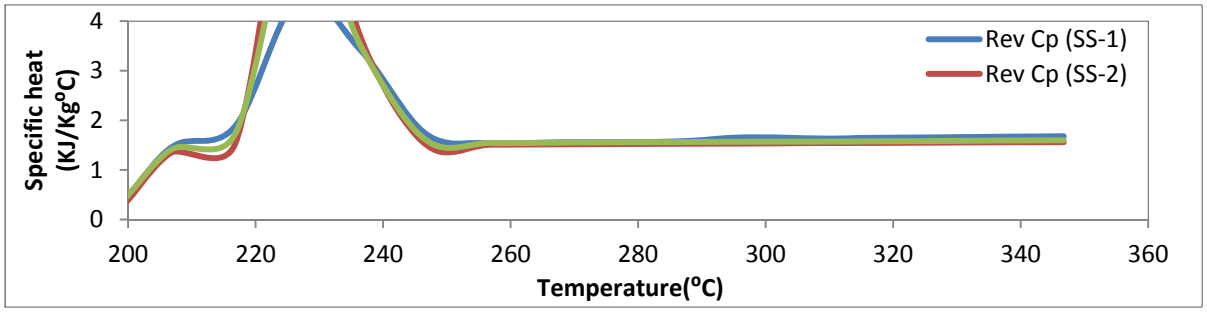

Figure 3.1 Specific heat capacity of Solar Salt

The experimental results shows that the specific heat capacity of solar salt is 1.55(kJ/kg°C) which matches the reference value.

3.1.2 Specific heat capacity by SDSC

Table 3.2 Results of Specific heat capacity by SDSC

Heat capacity(kJ/kg°C)	**$NaNO_3$-KNO_3(SOLAR SALT)**	
Heat capacity	**Experimental**	**Reference[20]**
Repeat #1	**1.61**	**1.45-1.55**
Repeat #2	**1.62**	
Repeat #3	**1.62**	
Average	**1.61**	
Standard deviation	**0.01**	

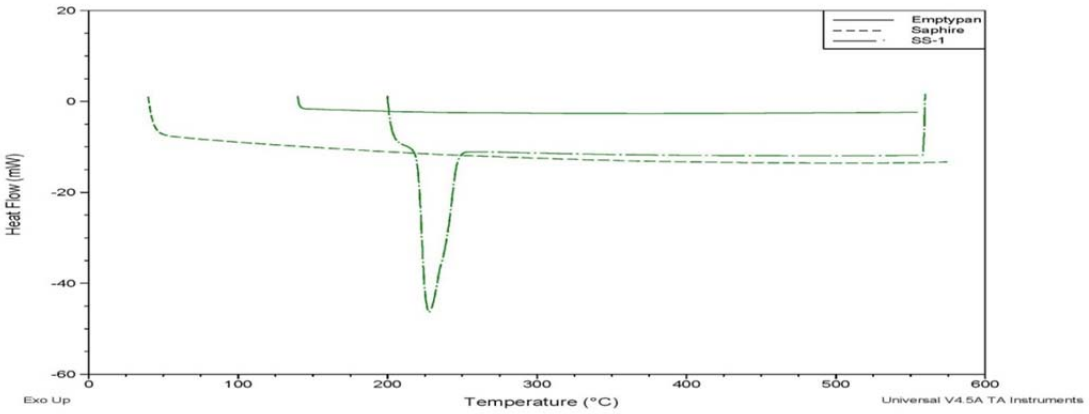

Figure 3.2 Raw data for Specific heat capacity measurement of Solar Salt

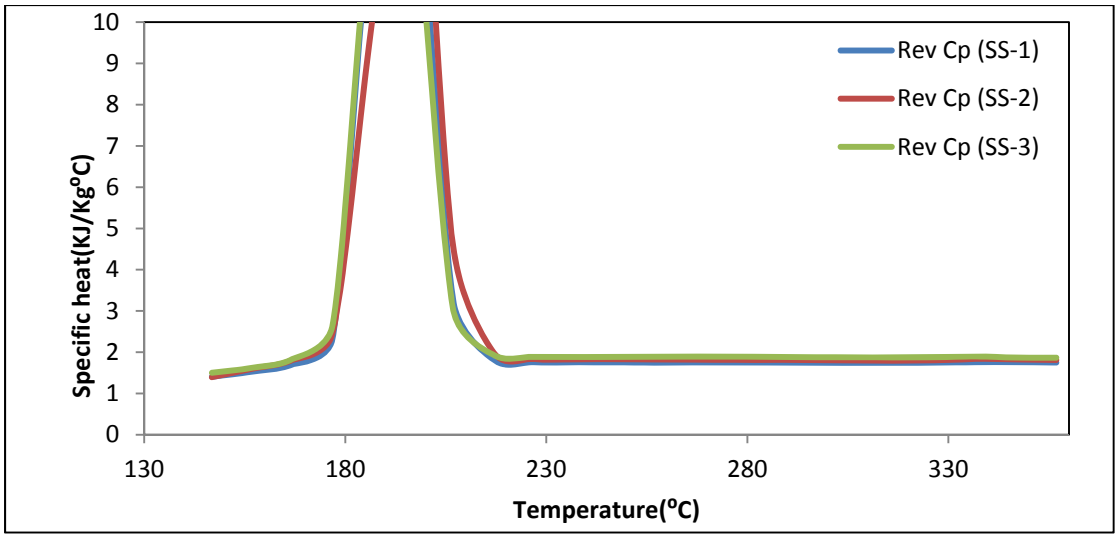

Figure 3.3 Processed data for Specific heat capacity measurement of Solar Salt

The experimental results shows that the specific heat capacity of solar salt is 1.61(kJ/kg°C) which is greater than the reference value. This error might be due to high ramping temperatures or improper placement of pan in the DSC cell (that is the surface contact of the pan and cell).

3.1.3 Specific heat capacity by T-History method:

The specific heat is calculated by using following equation[21,22]

$$\left(\frac{c_{p,\text{sample}}}{c_{p,\text{ref}}}\right)_{@\,Ts} = \frac{(dT_{\text{ref}}/dt)_{@\,Ts} \cdot (T_{air} - T_{\text{sample}})_{@\,Ts}}{(dT_{\text{sample}}/dt)_{@\,Ts} \cdot (T_{air} - T_{\text{ref}})_{@\,Ts}}$$

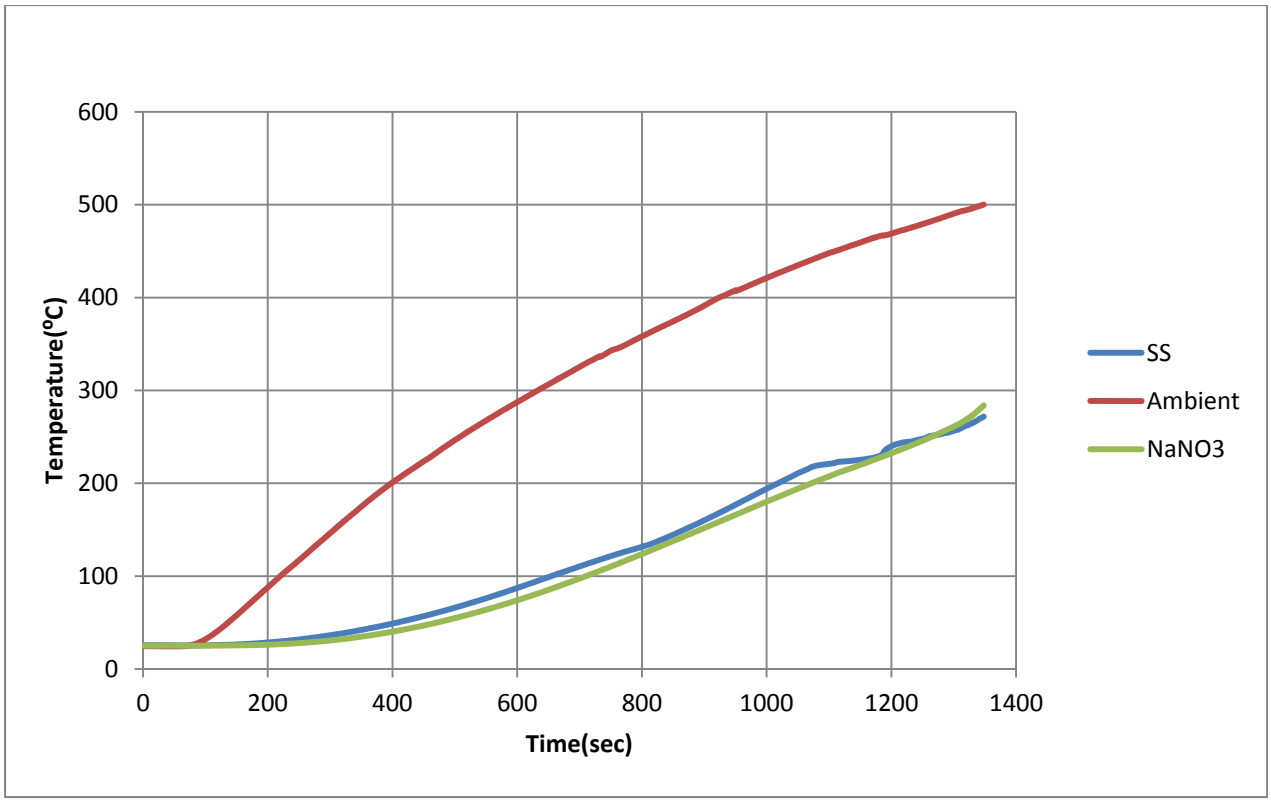

Figure 3.4 Time VS Temperature plot for SS, Ambient and $NaNO_3$

SS=Solar salt

Ambient=Furnace air temperature

$NaNO_3$=Sodium nitrate

Under same convective heating condition, the solar salt salt sample (with smaller c_p) heats up faster than the $NaNO_3$ sample heats (with large c_p).

Table 3.3 Results of Specific heat capacity by T-History

Heat capacity(kJ/kg°C)	**$NaNO_3$-KNO_3(SOLAR SALT)**	
Heat capacity	**Experimental**	**Reference[20]**
Repeat #1	**1.78**	**1.45-1.55**
Repeat #2	**1.76**	
Repeat #3	**1.75**	
Average	**1.76**	
Standard deviation	**0.01**	

The experimental results shows that the specific heat capacity of solar salt is 1.76(kJ/kg°C) which is greater than the reference value. This error might be due to improper placement of thermocouples inside the vials the advantage of this method is that it's cost effective and it can be used to find specific heat in bulk quantity whereas DSC is used only for small sample amounts.

3.2 Specific Heat capacity results of nitrate salts

The result from the SDSC gives the specific heat enhancement for the particular sample. The specific heat capacity is measured with SDSC since according to guidelines of Texas instrumentation if new sample is tested for specific heat SDSC should be used . The pure sample are tested first followed by the nanoparticles. The comparison is completely

evaluated in the liquid state. Pure samples are prepared in large number and are tested individually. The mean of the specific heat capacity that is measured is fixed to be the standard and it is close with the literature value from earlier experiments. The mean obtained from the experiments is close to about 1.8 KJ/KgºC and the literature value for is close to 1.89 KJK/gºC. The standard deviation is measured for the values obtained with repeated testing of the pure salt. The standard deviation gives the measure of the deviation between the mean and the expected value.

Table 3.4 Results of Specific heat capacity of Pure LiNO_3-NaNO_3

Heat capacity(kJ/kg°C)	**Pure LiNO_3-NaNO_3**	
Heat capacity	**Experimental**	**Reference[24-25]**
Repeat #1	**1.74**	**1.89**
Repeat #2	**1.8**	
Repeat #3	**1.87**	
Average	**1.8**	
Standard deviation	**0.07**	

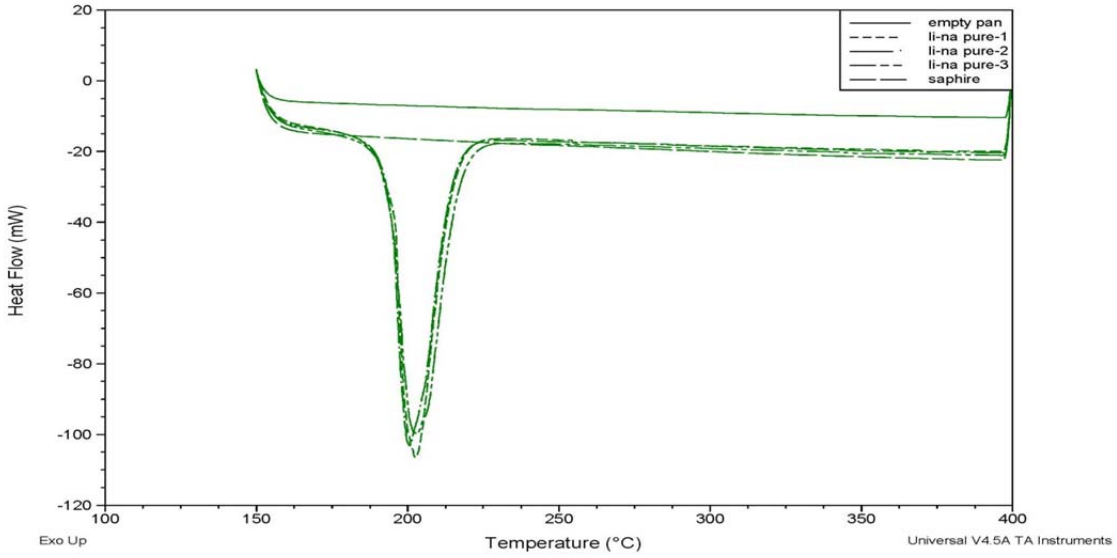

Figure 3.5 Raw data for Specific heat capacity of Pure LiNO_3-NaNO_3

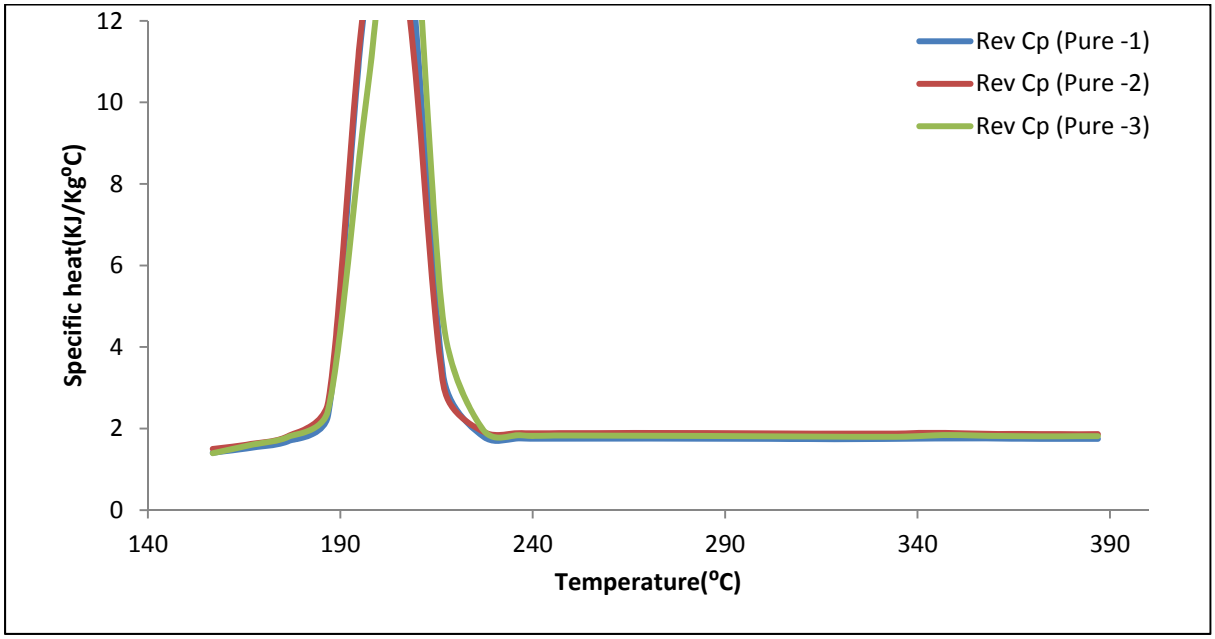

Figure 3.6 Processed data for Specific heat capacity of Pure LiNO_3-NaNO_3

Table 3.5 Results of Specific heat capacity of LiNO_3-NaNO_3-Al2O_3

Heat capacity(kJ/kg°C)	**LiNO_3-NaNO_3-Al2O_3**
Heat capacity	**Experimental**
Repeat #1	**2.06**
Repeat #2	**2.21**
Repeat #3	**2.11**
Average	**2.13**
Standard deviation	**0.08**

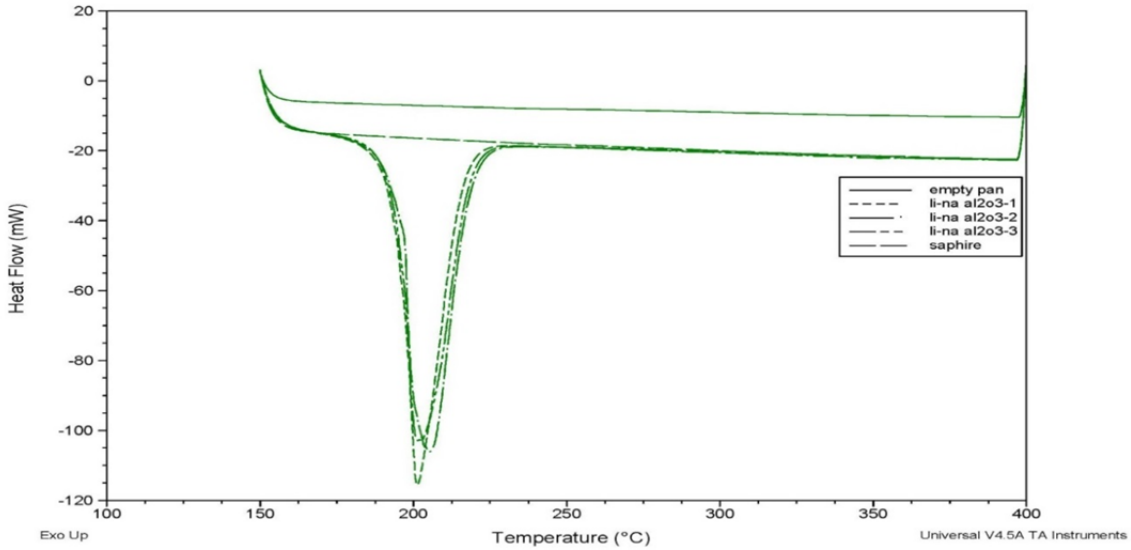

Figure 3.7 Raw data for Specific heat capacity of LiNO_3-NaNO_3-Al2O_3

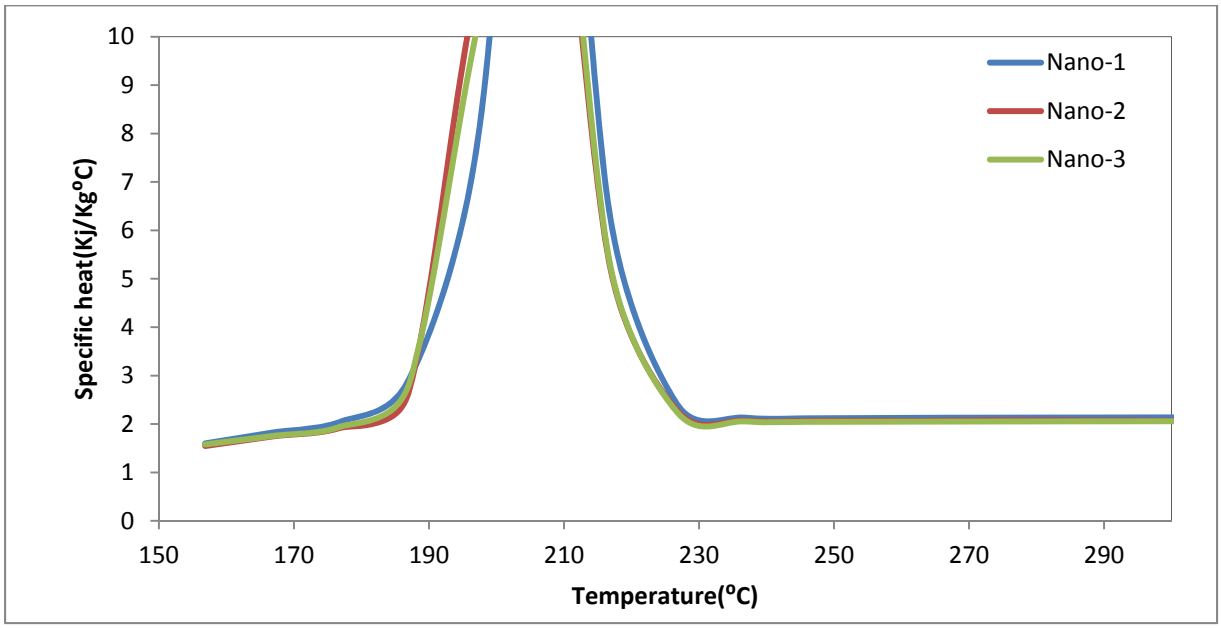

Figure 3.8 Processed data for Specific heat capacity of LiNO_3-NaNO_3-Al2O_3

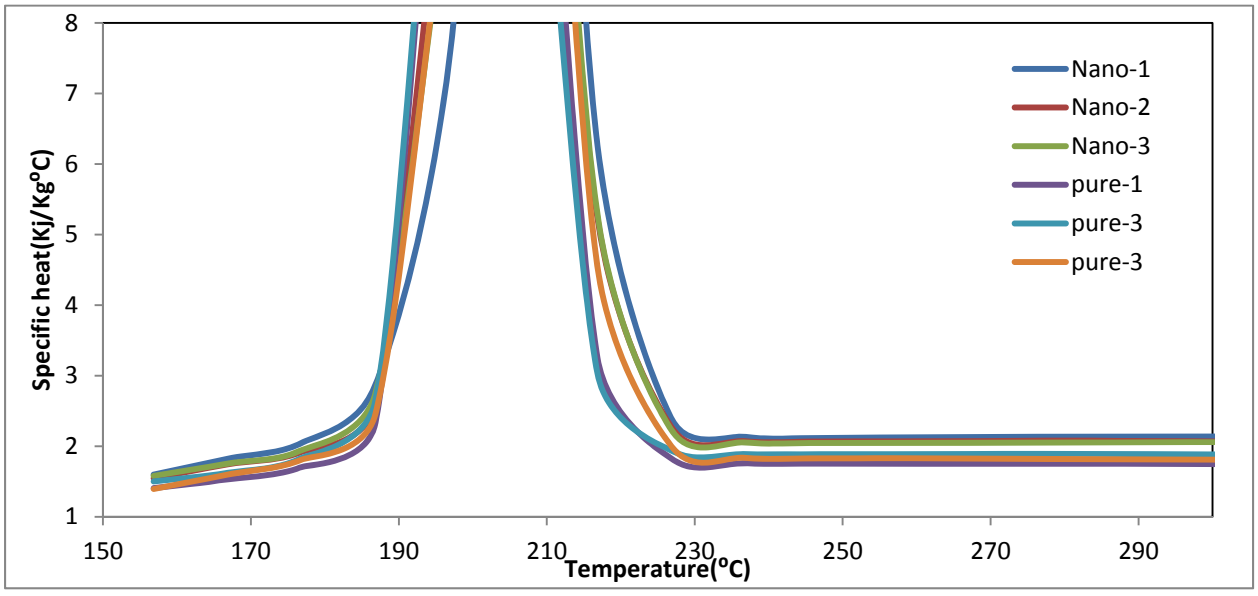

Figure 3.9 Processed data for Specific heat capacity of Nano VS pure

3.3 Proposed Mechanisms of enhanced specific heat capactiy of nanofluid

According to literature the specific heat enhancement might be due to three independent competing inter-molecular interaction mechanisms (or modes) [17].

3.3.1 Mode I (Enhanced specific heat capacity of nanoparticle due to higher specific surface energy):

Literature reports show that the specific heat capacity of particles can be enhanced up to 25% (compared to bulk property values) due to the high surface energy per unit mass of the nanoparticle. The surface atoms in the lattice of the nanoparticle are less constrained due to the less number of bonds. Since the bonds can be ‘‘visualized’’ to act like springs – the surface atoms vibrate at a lower natural frequency and higher amplitudes – resulting in higher surface energy. Hence, the phonon spectrums of nanoparticles are quantized and have discrete values which are constrained by the size of the nanoparticle[17].

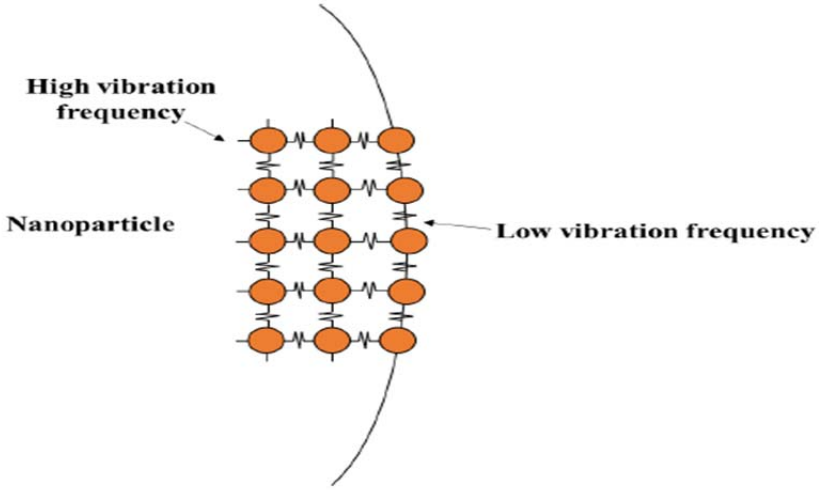

Figure 3.10 Mode I

3.3.2Mode II (Solid–Fluid interaction energy):

Extremely high surface area per unit mass of nanoparticles cause an anomalous increase in the interfacial thermal resistance between the nanoparticles and surrounding liquid molecules, which is usually negligible in macro scale. This high interfacial thermal resistance should act as additional thermal storage due to the interfacial interaction of the vibration energies between nanoparticle atoms and the interfacial molecules[17].

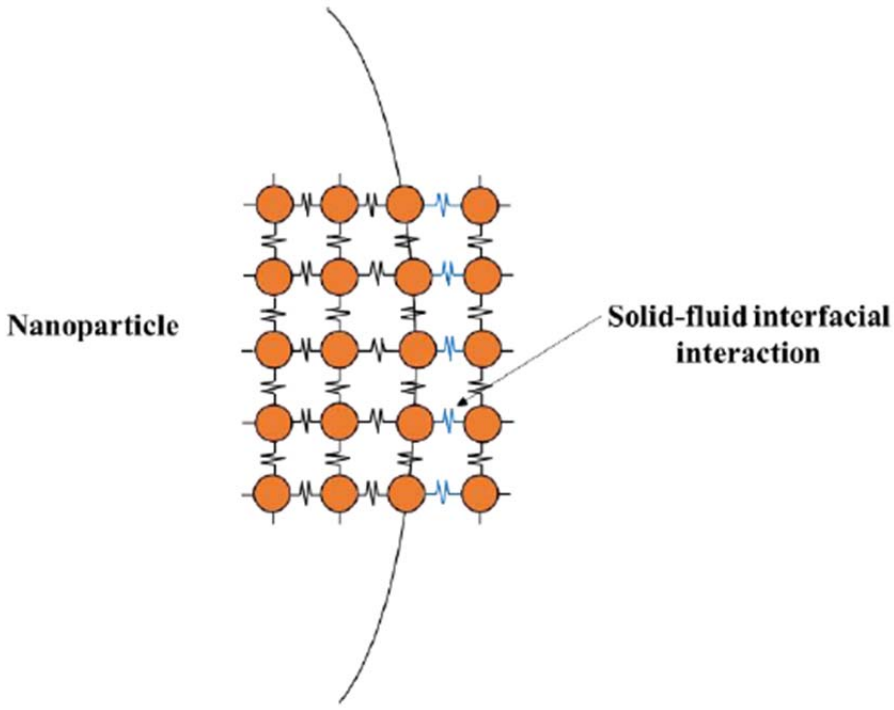

Figure 3.11 Mode II

3.3.3Mode III (Layering of liquid molecules at surface to form semi-solid layer):

In addition, liquid molecules adhering on the surface of the nanoparticles have a semi-solid behavior. The thickness of this ‘‘adhesion layer’’ of liquid molecules would depend on the surface energy of the nanoparticle. These semi-solid layers usually have higher thermal properties than the bulk liquid and therefore contribute to increasing the effective specific heat capacity of nanofluid[17].

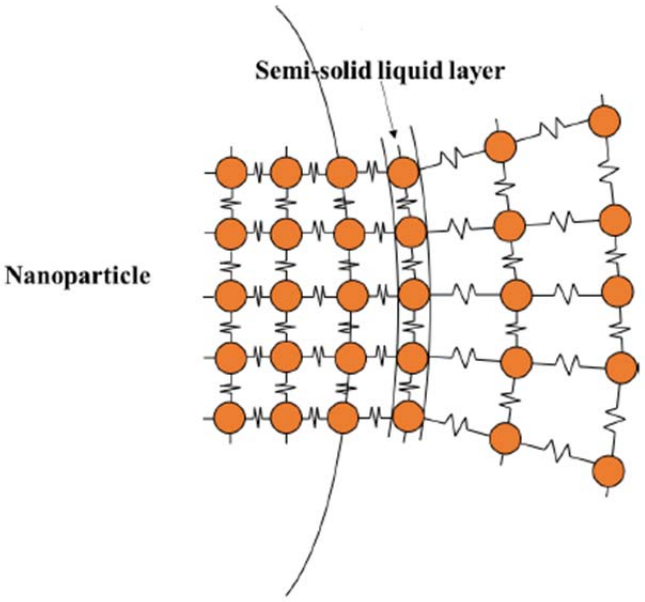

Figure 3.12 Mode III

3.4 Economic analysis of specific heat enhancement in CSP

Table 3.6 SAM Validation with respect to literature[18]

Validation of model			
Metric	SAM Value	Reported value	Difference(%)
Annual Energy	107,354,640kWh	110,000,000 kWh	2.4%
Capacity Factor	70.4%	74%	3.6%
Total Land Area	438.18 acres	457.00 acres	4.1%

The simulation gave energy output of approximately 107.4 GWh/year. The reported output for Gemasolar is estimated at 110 GWh/year from literature, giving a 2.4% difference in the actual and simulated values. 4.1% difference was found in between the simulated and reported values for the total land of the plant. The specific heat enhancement values shown in below table are obtained from the literature

Table 3.7 Enhancement of specific heat of nanoparticle size with respect to literature

Enhancement of specific heat based on nanoparticle size[20]				
Base salt	$NaNO_3$-KNO_3	$NaNO_3$-KNO_3	$NaNO_3$-KNO_3	$NaNO_3$-KNO_3
Nanoparticle	SiO2	SiO2	SiO2	SiO2
Nanoparticle size	5nm	10nm	30nm	60nm
Enhancement	10%	13%	21%	28%

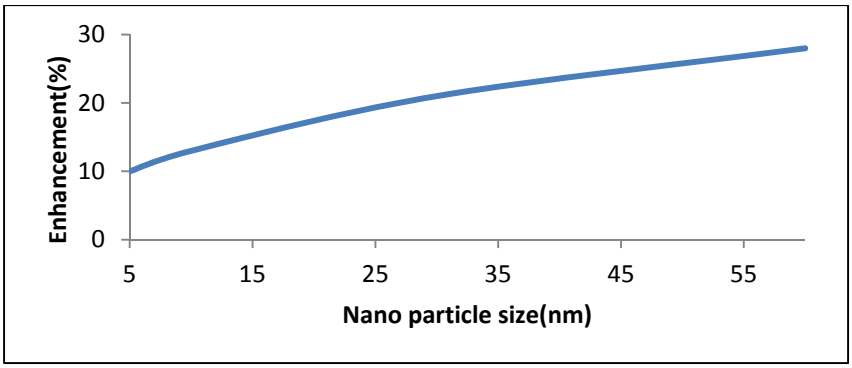

Figure 3.13 Performance of Nano particle size VS Enhancement

Table 3.8 TES cost with respect to enhancement[16,19]

Cp Enhancemnt(%)	TES cost($/Kg)
0	26.22
10	24.12
13	23.17
21	21.8
28	20.71

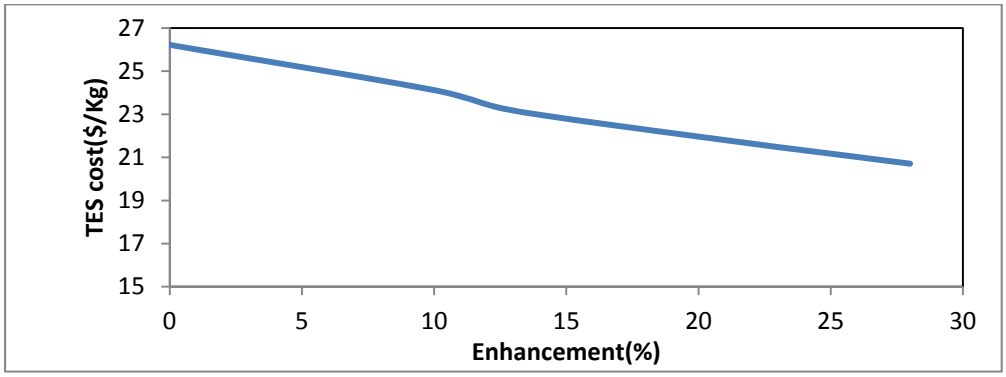

Figure 3.14 Performance of Enhancement VS TES costs

Table 3.9 Over all TES cost with respect to enhancement

Cp Enhancement(%)	Over all Installation TES cost reduction (%)
0	**-**
10	**8**
13	**11.6**
21	**16.5**
28	**21.02**

As the specific heat increases there will be reduction in thermal energy storage cost this might be due to due to reduction of insulation , construction cost of tanks, smaller tank size.

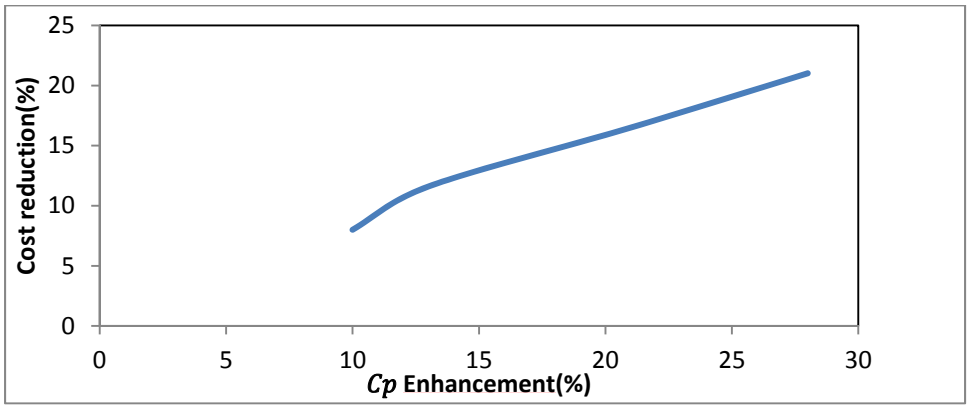

Figure 3.15 Performance of C_p Enhancement VS cost reduction

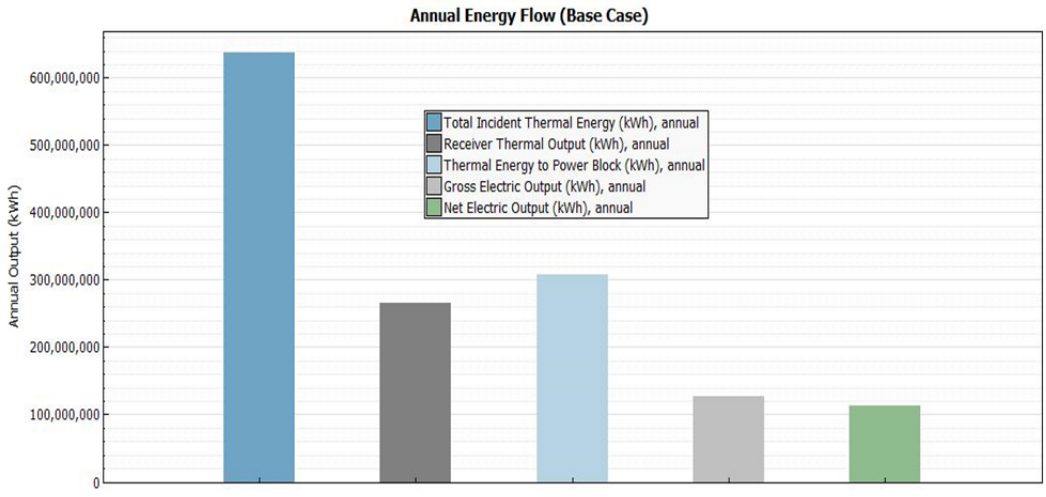

Figure 3.16 The annual energy flow of different processes in the system

The above graph depicts the annual energy based on difference losses from different processes throughout the system in concentrated solar power plant.

CHAPTER 4

CONCLUSION AND FUTURE WORK

4.1 Conclusion

In this study different methods of specific heat measurement techniques has been performed for solar salt to find its heat capacity and MDSC showed the heat capacity equal to that of reference value, binary nitrate salt eutectic ($LiNO_3$–$NaNO_3$, 54:46 mol. %) doped with Alumina nanoparticles (1% wt., 40nm) is investigated as a potential candidate to be used in thermal energy storage media in concentrated solar power systems. Specific heat capacity (C_p) measurement is performed using a modulated differential scanning calorimeter. The result of the specific heat analysis shows 18.3% $C_p$enhancement compared with the pure salt eutectic. The enhanced specific heat capacity of a TES fluid can significantly reduce the material and structure cost of TES in a CSP system. The economic impact on the effect of specific heat capacity enhancement has been conducted by using System Advisor model for simulation. It was proven that by enhancing specific heat of 10%, 13%, 21%, 28% we can reduce the overall cost of TES about 8%, 11.6%, 16.5%, 21.02%.

4.2 Future work

The future work for the binary nitrate mixture can be as following:

1. Verifying the Thermal and Chemical Stability at higher temperatures.
2. Viscosity measurement.
3. Checking the effect of additional nitrate with the base salt like ternary or quaternary nitrate mixtures.

References

[1] Thomas, L. C. Modulated DSC Paper #1 Why Modulated DSC? An Overview and Summary of Advantages and Disadvantages Relative to Traditional DSC. TA Instruments Technol. Pap. 2005, TP,006.

[2] Ylenia Cascone, Marco Perino, " Estimation of the thermal properties of PCMs through inverse Modelling," IBPC 2015.

[3] M. Reading, A. Luget, R. WilsonModulated differential scanning calorimetry Thermochim Acta, 238 (1994), pp. 295-307

[4] A. Boller, Y. Jin, B. Wunderlich J. Therm. Anal, 42 (1994), pp. 307-330.

[5] P. S. Gill, S. R. Sauerbrunn and M. Reading," MODULATED DIFFERENTIAL SCANNING Calorimetry", Journal of Thermal Analysis), pp. 931-939.

[6] Chu, Y. (2011). Review and comparison of different solar energy technologies. Global Energy Network Institute (GENI), August.

[7] A. Shah, P. Torres, R. Tscharner, N. Wyrsch and H. Keppner, "Photovoltaic technology: the case for thin-film solar cells," science, vol. 285, no. 5428, pp. 692-698, 1999.

[8] C. Harmon, "Experience curves of photovoltaic technology," Laxenburg, IIASA, vol. 17, 2000.

[9] Concentrated Solar Power.

[10] R. Guerrero-Lemus and J. M. Martnez-Duart, "Concentrated Solar Power," in Renewable Energies and CO2, Springer, 2013, pp. 135-151.

[11] H.L.Zhang,J.Baeyens,.Degrève,G.Cacères, " Concentrated solar power plants: Review and design methodology" June 2013, Pages 466-481.

[12] Rebecca I. Dunn, Patrick J. Hearps, and Matthew N. Wright, "Molten-Salt Power Towers: Newly Commercial Concentrating Solar Storage".

[13] Tomislav M.PavlovićIvana S.RadonjićDragana D.MilosavljevićLana S.Pantić, "A review of concentrating solar power plants in the world and their potential use in Serbia", August 2012, Pages 3891-3902.

[14] D. Shin, D. Banerjee, Enhancement of specific heat capacity of high-temperature silica nano fluids synthesized in alkali chloride salt eutectics for solar thermal-energy storage applications, International Journal of Heat and Mass Transfer 54 (2011) 1064-1070.

[15] H. Tiznobaik, D. Shin, Experimental validation of enhanced heat capacity of ionic liquid based nanomaterial, Applied Physics Letters (in press).

[16] Malik, D., "Evaluation of Composite Alumina Nanoparticle and Nitrate Eutectic Materials for Use in Concentrating Solar Power Plants." Thesis, Texas A&M University, College Station TX, 2010.

[17] Donghyun Shin, Debjyoti Banerjee," Enhancement of specific heat capacity of high-temperature silica-nanofluids synthesized in alkali chloride salt eutectics for solar thermal-energy storage applications", International Journal of Heat and Mass Transfer 54 (2011) 1064–1070.

[18] Fuentes De Andalucía," System Advisor Model (SAM) Case Study",NREL.

[19] Glatzmaier, G. (2011). Summary Report for Concentrating Solar Power Thermal Storage Workshop: New Concepts and Materials for Thermal Energy Storage and Heat-Transfer Fluids, May 20, 2011 (No. NREL/TP-5500-52134). National Renewable Energy Laboratory (NREL), Golden, CO.

[20] Dudda, B., & Shin, D. (2013). Effect of nanoparticle dispersion on specific heat capacity of a binary nitrate salt eutectic for concentrated solar power applications. International journal of thermal sciences, 69, 37-42.

[21] E. R. G. Eckert and R. Drake, Analysis of Heat and Mass Transfer, McGraw–Hill, New York, 1972.

[22] J. P. Holman, Heat Transfer, Ninth edition, McGraw–Hill, New York, 2002.

[23] ASTM Standard E1269, 2005, “Standard Test Method for Determining Specific Heat Capacity by Differential Scanning Caloimetry,” ASTM Internatiional, West Conshohocken, PA, 2005, DOI: 10.1520/E1269-05, www.astm.org.

[24] Olivares, Rene I., Chunlin Chen, and Steven Wright. "The thermal stability of molten lithium–sodium–potassium carbonate and the influence of additives on the melting point." Journal of solar energy engineering 134.4 (2012): 041002

[25] Wu, Yu-ting, et al. "Experimental study on optimized composition of mixed carbonate salt for sensible heat storage in solar thermal power plant." Solar Energy 85.9 (2011): 1957- 1966.

Biographical Information

Vamsikiran Eruvaram was born in Chittoor,Andhra Pradesh, India on 18th August 1995. He did his schooling in Vignana deepthi English medium school. He graduated from Sri Vidyanikethan Engineering college (Jawaharlal Nehru Technological University Anantapur) in 2016 with Bachelor of Technology in Mechanical Engineering; during Bachelors he worked as an intern for two companies. In May 2018 he completed his Master of Science degree in Mechanical Engineering from the University of Texas at Arlington. He has over 2 years of experience in thermal fabrication of novel molten salt for energy storage material whose application lies in concentrated solar power plant. He also holds expertise in Material characterization techniques such Scanning Electron Microscopy and Energy Diffusive Spectroscopy. During his Master's he worked as Intern in Lennox International as Mechanical Engineer for around 5 months in product development and research sector.

Vamsikiran Eruvaram is the eldest son to Mr. Surendra Reddy Eruvaram and Mrs. Chamundeswari Kothoor. His elder sister Mrs. Madhuri Mounika Eruvaram is working as Electrical Engineer at GENCO.